Electron-microprobe study of chromitites associated with alpine ultramafic complexes and some genetic implications

by

M.L. Bird

U.S. Geological Survey

Reston, Virginia 22092

Open-File Report No. 78-119

1978

Electron-microprobe study of chromitites associated with alpine ultramafic complexes and some genetic implications

M.L. Bird

Abstract

Electron-microprobe and petrographic studies of alpine chromite deposits from around the world demonstrate that they are bimodal with respect to the chromic oxide content of their chromite. The two modes occur at 54 ± 4 and 37 ± 3 weight per cent chromic oxide corresponding to chromite designated as high-chromium and high-aluminum chromite respectively. The high-chromium chromite occurs exclusively with highly magnesian olivine (Fo92-97) and some interstitial diopside. The high-aluminum chromite is associated with more ferrous olivine (Fo88-92), diopside, enstatite, and feldspar.

The plot of the mole ratios Cr/(Cr+Al+Fe3+) vs Mg/(Mg+Fe2+) usually presented for alpine chromite is shown to have a high-chromium, high-iron to low chromium, low-iron trend contrary to that shown by stratiform chromite. This trend is characteristic of alpine type chromite and is termed the alpine trend.

However, a trend similar to that for stratiform chromite is discernable on the graph for the high-chromium chromite data. This latter trend is well developed at Red Mountain, Seldovia, Alaska.

Analysis of the iron-magnesium distribution coefficient, Kd=(Fe/Mg)ol/(Fe/Mg)ch, between olivine and chromite shows that Kd for the high-chromium chromite from all ultramafic complexes has essentially the same constant value of .05 while the distribution coefficient for the high-aluminum chromite varies with composition of the chromite. These distribution coefficients are also characteristic of alpine-type chromites. The constant value for Kd for the high-chromium chromite and associated high-magnesium olivine in all alpine complexes suggests that they all crystallized under similar physico-chemical conditions.

The two types of massive chromite and their associations of silicate minerals suggest the possibility of two populations with different origins. Recrystallization textures associated with the high-aluminum chromite together with field relationships between the gabbro and the chromite pods, suggest that the high-aluminum chromite was formed by metamorphic recrystallization of the ultramafic rocks and adjacent gabbro.

Contents

List of illustrations

5. Variation in the weight per cent of the component oxides of the alpine chromite at Red Mountain, Seldovia, Alaska as a function of chromic oxide content of the chromite.
6. Graph of Cr/(Cr+Al+Fe3+) vs Mg/(Mg+Fe2+) for all alpine chromite analyzed in this study except Red Mountain Alaska.
7. Graph of Cr/(Cr+Al+Fe3+) vs Mg/(Mg+Fe2+) for chromite of the Red Mountain alpine ultramafic complex at Seldovia, Alaska.
8. Photograph of specimen of olivine chromitite which has a reaction zone of pyroxene and spinel adjacent to an intrusive feldspar dikelet.
9. Histograms of the frequency of occurrence of alpine chromite deposits which contain chromite with different percentages of chromium oxide.
10. Graph of (Cr/Al)/di vs (Cr/Al)/ch for chromite-diopside pairs from alpine chromitites. The gap in the data at (Cr/Al)ch = 2.2-2.3 lies between high chromium and high aluminum chromite.
11. Graph of (Fe/Mg)ol vs (Fe/Mg)ch for all olivine-chromite pairs analyzed in study with the exception of those from Red Mountain, Seldovia, Alaska.

Introduction

Deposits of chromite associated with alpine-type ultramafic complexes are of economic interest both for high-chromium and low-chromium (high-aluminum) ores. The high and low-chromium ores correspond, in general, to metallurgical and refractory grade ores which by definition must contain more than 45 and a minimum of 31 weight per cent Cr_2O_3 respectively (NMAB, 1970).

The purpose of this study is to investigate the relationships between high-chromium and low-chromium, high-aluminum, chromites and their associated silicate minerals in alpine-type ultramafic rocks with the goal of understanding their genesis.

Comparison of some characteristics of alpine-type deposits with those of stratiform chromite deposits is made in order to provide a firmer basis for interpretation of the analytical results obtained in this study.

Alpine-type chromite occurs as podiform and lens shaped segregations and as disseminated grains scattered throughout massive dunites and peridotites which have been partially serpentinized. The dunites and peridotites, together with their contained chromitites, are component parts of what is referred to as an ophiolite suite of rocks which, when all components are

present, is composed of an ultramafic section overlain by gabbro, basalt, pillow lavas, and tuffaceous and cherty sedimentary rocks. Because of the occurrence of ophiolites as tectonically emplaced fault blocks, their composition, and widespread occurrence, especially along island arcs, they are thought to represent fragments of the uppermost mantle and immediately overlying crust (Davies, 1971; Coleman, 1971).

Among the first detailed field and petrographic studies of chromite were those of Sampson (1929, 1931, and 1932) who classified chromite deposits as being of primary or secondary origin although at that time no distinction was made between the alpine and stratiform types.

In field studies of chromite deposits in Cuba, Thayer (1943) pointed out that in several provinces the chromite deposits were in peridotites closely associated with gabbroic rocks. Thayer (1963) later observed that all podiform chromite deposits occur with either dunite or troctolite as gangue, halos, or country rock.

Similarly, other investigators (Flint and others, 1948; Stoll, 1958; Smith, 1958; MacGregor and Smith, 1962; and Rossman, 1959, 1970) have described the close spatial association of the chromite deposits to the peridotite-gabbro contact in ophiolite sequences.

Thayer (1969, 1970) proposed that the dunites and peridotites of alpine ultramafic complexes were formed by crystallization and sedimentation from a magmatic melt. Most alpine ultramafic bodies, however, have been sufficiently deformed and recrystallized by dynamic metamorphism to obscure the primary layering, cross-bedding, and other features indicative of such an origin. This is the case with most of the complexes included in this study.

Recent studies of alpine complexes (Irvine and Findlay, 1971; Dewey and Bird, 1970; Moores, 1969; Lanphere, 1973, Jackson and others, 1974) indicate that the ultramafic section is generally unconformable with the overlying mafic section and, in some cases at least, an ultramafic differentiate of the mafic rock lies on top of the ultramafic section. With this interpretation the lowermost ultramafic section is usually more extensively deformed and is referred to as a tectonite (Jackson and others, 1974).

Samples and methods of present study

Samples and preparation--Many of the samples studied in this investigation are from a large collection of alpine chromitites collected by T.P.Thayer from world-wide occurrences of alpine ultramafic complexes such as Twin Sisters, Washington; Canyon Mountain, Oregon; Tiebaghi, New Caledonia; Guleman, Turkey; Zambales, Philippine Islands; Dun Mountain, New Zealand; Camaguey, Cuba; Troodos, Cyprus; Niquelandia, Brazil; Webster-Addie and Dark Creek, North Carolina; and others. Each sample from Thayer's collection represents a chromite concentration or mine and any "accessory" chromite is generally in the same hand specimen as more massive chromite. Many of the ultramafic complexes are represented by a single specimen. Samples from the Coolac belt, Australia, were obtained from H.G.Golding and those from Eklutna, Claim Point, and Red Mountain, Alaska were collected by A.L. Clark and P.W. Guild. Many of the samples from the Red Mountain complex were collected along traverses planned in regard to lithologic variations and include both massive and accessory chromite. The data from the Red Mountain complex, therefore, are treated separately.

Standard polished sections and polished thin sections were prepared of all hand specimens. Each section was examined petrographically and areas were selected for electron microprobe analysis. In the area selected for microprobe analysis, central, unaltered points on crystals of chromite were analyzed to obtain representative chromite compositions. Both central points and points near the edges of each chromite grain and adjacent silicate minerals were analysed to determine variations within and between phases. In many specimens microprobe traverses were made across grains and grain boundaries.

Method of microprobe analysis--Electron microprobe analyses were made with an ARL-EMX-SM microprobe having three spectrometers equipped with ADP, LiF, and RAP crystals. Operating conditions used were an accelerating potential of 15 kV and a beam current of 0.1 ma. The beam current was integrated over 2.0 ma for a counting time of approximately 20 seconds. The x-ray counts for each of the elements Ca, Cr, Al, Si, Fe, Mg, Ti, Ni, and Na were determined three at a time, in the order given, at each of point of analysis. After analyzing many points for three elements the spectrometers were reset and standardized for the next three elements and the same point was re-occupied with the beam. Re-occupying

the same point was facilitated by the use of microphotographs and the mark left by the beam. Duplicate reading were made at each analyzed point and the data were corrected using the procedures described by Sweatman and Long (1969).

Standards for microprobe analysis included a chemically analyzed chromite from Union Bay, Alaska for the elements Cr, Fe, Ti, and Ni. Synthetic enstatite was the standard for Mg and Si and synthetic anorthite was used for Ca and Al. For quality control chemically analysed chromites from the Stillwater complex, Montana were analyzed as unknowns during each period of analysis.

Calculations of the weight per cent of FeO and Fe_2O_3 from total iron in chromite was made by setting the total number of moles of the divalent metal ions to 1.000 and recalculating the remaining iron as Fe_2O_3.

Petrography of the Analyzed Chromitites--The chromitites analyzed in this study consist of the minerals chromite, olivine, pyroxene, and feldspar in varying proportions. The olivine is generally anhedral and either has a fine, equigranular texture or contains large recrystallized grains which are irregular in outline and show undulatory extinction and glide twinning. Where the bedding planes are discernable by other criteria such as layers of cumulate chromite, the recrystallized olivine grains are generally oriented at an angle to the bedding planes. In some complexes such as Canyon Mountain, Oregon, large grains of olivine with euhedral outlines are present.

If olivine is the only silicate mineral present, the associated chromite grains are commonly euhedral to subhedral and are dark reddish brown in thin section. This chromite is a high-chromium variety. If the olivine is deformed and oriented at an angle to the original cumulate layering, the chromite grains may also be rounded and aligned along the metamorphic fabric developed in the silicates.

The pyroxenes consist of diopside and enstatite which may contain exsolution lamellae of one another and which have undulatory extinction, twinning, and well developed cleavage. The cleavages are parallel to the

110 plane (210 in enstatite) and the exsolution lamellae and twinning are parallel to the 100 plane in both ortho- and clinopyroxene.

Where the associated silicate minerals are pyroxene, olivine, and feldspar, the chromite is commonly anhedral and is high in alumina and low in chromium. Some chromite is frequently developed as hooks and stringers along the feldspar-olivine contacts (fig.1). A similar reaction relationship is shown by fig.2 in which enstatite , diopside (not shown), and enstatite are developed between olivine and feldspar. The chromite which is associated with pyroxene (and olivine) usually has globular outlines and is molded around olivine and pyroxene crystals giving the general appearance of metamorphic relics and recrystallization texture similar to that described by Sampson, 1929 (figs. 3 and 4). Figures 3 and 4 also show crystals of chromite (with altered olivine inclusions) with a higher Cr_2O_3 content (44%) serving as nuclei around which the low chromium chromite (36% Cr_2O_3) precipitated.

Although the ultramafic complex at Red Mountain, Seldovia, Alaska shows little megascopic evidence of intensive dynamic metamorphism, recrystallization is evident among the silicate minerals. In ultramafic complexes such as Canyon Mountain, Oregon and the

Zambales complex, Philippine Islands, however, where intensive dynamic metamorphism is evidenced by folding, cataclastic textures are not normally present and undulatory extinction is not as prevalent as at Red Mountain, Alaska.

Chemistry of chromite

The mineral chromite belongs to the spinel group of minerals and consists of a solid solution of $FeCr_2O_4$, chromite (sensu stricto), $MgCr_2O_4$, $FeAl_2O_4$, $MgAl_2O_4$, $FeFe_2O_4$, $MgFe_2O_4$, and contains minor amounts of other elements. It thus has the general formula AB_2O_4 in which A represents one or more of the divalent metals (Fe^{2+}, Mg, Ni, Co, Mn, Zn), B is one or more of the trivalent metals (Fe^{3+}, Al, Cr) or Ti^{4+}, and O is oxygen. The dominant metals (ions) are Fe^{2+}, Mg, Cr, Al, and Fe^{3+}, hence the formula $(Fe^{2+},Mg)(Cr,Al,Fe^{3+})_2O_4$ in which all cations occur in varying proportions.

Analytical Results

Microprobe analyses of alpine chromite--The electron microprobe analyses for this study have been prepared as a U.S. Geological Survey open-file report (Bird, 1977). The analyses show very little primary variation in composition within the chromite grains in podiform deposits associated with dunite. The small changes which were observed are confined to one or two microns from grain edges and usually are different in chromite adjacent to olivine and chromite adjacent to pyroxene or other minerals. These small variations thus appear to reflect solid-solid equilibration with the enclosing silicate minerals. Variations between adjacent grains and between accessory chromite and massive chromite in the same hand specimens and same deposits are usually only 1 to 2 per cent Cr_2O_3 and Al_2O_3. Variations between deposits in an ultramafic complex such as Canyon Mountain, Oregon, however, are significant and provide much of the data for the conclusions of this study. The Cr_2O_3 content of massive chromite in all deposits studied was found to be either 54% ± 4% or 37 ± 3% (weight per cent).

Microprobe analyses of chromite in a feldspathic gangue may show, in some deposits, variations within individual grains of as much as 50% of the amount of Cr_2O_3 present with corresponding reciprocal variations in Al_2O_3. These variations, however, are limited to rims of late chromite rimming the chromite and olivine grains along olivine-feldspar interfaces such as the hooks and stringers of fig.1.

The analyses (Bird, 1977) show that alpine type chromite is characterized by 1) reciprocal variations between chromium and aluminum content from about 1.5 moles Cr to less than 0.5 mole Cr; 2) usually small quantities of Fe_2O_3; 3) reciprocal variation between Fe^{2+} and Mg from about 0.7 mole to 0.3 mole Mg; and 4) low concentrations of TiO_2 usually near 0.25 but varying to 0.75 weight per cent. The sum of the moles of the oxides of Fe^{2+} and Mg have been set equal to 1.000 (with minor amounts of Ni and Mn) and the moles of oxides of Cr, Al, and Fe^{3+} total 2.00 including some Ti and Si.

Variations in compositions of alpine-type chromite --Figure 5 shows the graph of Al_2O_3, MgO, and Fe_2O_3 plotted against Cr_2O_3 for the alpine chromite from Red Mountain, Seldovia, Alaska. The graph illustrates the rapid decrease in aluminum and slight increase in ferric iron as chromium increases. The plot of the ferric iron data shows a slight decrease in ferric iron as chromic oxide increases above 50%. Magnesium oxide decreases as chromic oxide increases up to near 50% and then increases as cnromic oxide continues to increase above 50%. The decrease in magnesium as chromium increases in alpine chromite which contains less than 50% chromic oxide is unique to alpine-type chromite and results in what is termed the alpine trend in this paper.

Cr/(Cr+Al+Fe3+) vs Mg/(Mg+Fe2+) trend in composition of alpine chromite--The plot of the mole ratio of Cr/(Cr+Al+Fe3+) against the mole ratio Mg/(Mg+Fe2+) for the chromite from each high grade alpine-type chromite deposit analyzed in this study is shown in fig.6. The resulting graph illustrates the high-chromium , low-magnesium to low-chromium, high-magnesium trend referred to as the alpine trend in the previous section. Published graphs of analytical data for alpine-type chromite, including accessory chromite, show the same trend (Loney and others, 1971; Irvine, 1965; Malpas and

Strong, 1975). Assuming that the alpine ultramafic rocks are formed by fractional crystallization from a magmatic melt and that the high chromium chromite is the first to crystallize, the chromite along the "alpine trend" becomes more magnesian and less ferrous as differentiation progresses. Analysis of the chromite data for individual complexes, however, shows that a high-chromium, high-magnesium to low-chromium, low-magnesium trend almost normal to the alpine trend can be discerned for the high-chromium chromite of alpine type. This trend is best exemplified by the high-chromium chromite data for the Red Mountain complex.

Figure 7 shows the graph of the mole ratios Cr/(Cr+Al+Fe7+) plotted against Mg/(Mg+Fe2+) for the massive and accessory chromite from Red Mountain. The part of the graph between points B and C has the trend which is characteristic of alpine chromite. As indicated in the figure, however, the data points which define the alpine trend (B-C) primarily represent accessory chromite. The open points (circles) represent accessory chromite from many different locations in the complex and the double circles represent accessory chromite in closely spaced samples (every two feet) from a stratigraphic section having a thickness of about 20 feet (6 m). For both symbols the points nearest point B

represent accessory chromite near a massive chromite layer and those nearest C represent chromite close to or in pyroxenite or peridotite layers. The chromite which is lowest in chromium is generally associated with minor enstatite, olivine, and diopside all of which have the highest content of iron. The open points between B and C generally represent accessory chromite in peridotite.

Other occurrences of low-chromium (high-aluminum) chromite in the Red Mountain complex lie adjacent to dikes of anorthitic feldspar (An90) which intrude the ultramafic section. This low-chromium chromite locally forms small massive bodies and apparently its low chromium content results from aluminum metasomatism and recrystallization of chromite adjacent to the feldspathic dikes. The composition of this chromite also plots along the characteristic alpine trend as is illustrated by the circled dots in fig.7.

Where dikes of feldspar intrude dunite a reaction zone consisting of pyroxene and spinel lies between the dunite and the feldspar (fig.8). Chromite in the dunite has a much higher chromium content and lower aluminum content than chromite near or in the reaction zone. The latter chromite apparently results from recrystallization (and partial substitution of Cr by Al)of the existing chromite. Texturally the chromite in or near the reaction zone is anhedral and much coarser than that in the dunite. The grains of olivine adjacent to the reaction zone also show evidence of recrystallization.

The graph between points A and B (fig.7) illustrates the high-chromium, high magnesium to low-chromium, low-magnesium trend referred to in previous paragraphs. The data points (dots) represent chromite in massive layers of cumulate chromite which consists of over 90 per cent chromite and less than 10 per cent olivine. The chromite in the high grade layers varies in composition from about 58 weight per cent chromic oxide in the denser parts of the layer to 49-50 weight per cent near the margins. The variations from 58 to 49 weight per cent Cr_2O_3 in the chromite is a primary compositional variation unrelated to changes which involve metasomatism.

Bimodality of alpine-type chromite

It is evident from fig.6 that the graphed data are divided into two fields that are at Cr/(Cr+Al+Fe2+) mole fractions of 0.7 and 0.4. An histogram of the frequency of occurrence of all the chromite deposits with different percentages of chromic oxide in the chromite are shown in fig.9a illustrating that the deposits are indeed bimodal with respect to the chromic oxide content of the chromite. The two modes occur at 54 and 37 weight per cent chromic oxide with standard deviations of 4 and 3 per cent respectively. These two modes are referred to as the high-chromium and low-chromium modes respectively.

The histograms for individual ultramafic complexes (figs.9b,c) illustrate that the bimodality of chromite deposits also occur in a single ultramafic complex.

Golding and Bayliss(1968) reported that the chromite deposits in the Coolac ultramafic belt of Australia are bimodal with respect to their Cr203 content and Golding and Johnson (1971) reported modes at 58 and 38 weight per cent Cr203 in the Coolac chromite deposits. Microprobe analyses of fifteen Coolac chromites in the present investigation have modes of 57 and 37 weight per cent Cr203 (fig. 9b). Similarly, the ultramafic complexes of Cuba and the Zambales

complex of the Philippine Islands contain chromite having a bimodal distribution. In both localities the chromite in dunite contains about 56 per cent chromic oxide and the chromite deposits which lie nearer the gabbro contain about 37 per cent chromic oxide.

The chromite deposits in the Canyon Mountain ultramafic complex, Oregon, are also bimodal (fig.9c). Mapping of the areal distribution of the Canyon Mountain chromite deposits illustrates a pattern of high chromium oxide deposits in the center of the complex which are surrounded by low-chromium chromite deposits adjacent to the pyroxenites and gabbros around the edges of the complex. Assuming the chromite to have been formed by continuous differentiation this pattern suggests that the chromite at the top of the ultramafic section is high in aluminum while the chromite from lower in the section is high in chromium. The alternative interpretation is that the high-aluminum chromite results from metamorphic recrystallization of the ultramafic section and adjacent gabbro. An abrupt difference between the two types of chromite is shown by the histogram of fig.9c.

The silicate minerals associations, which are distinguished by the different symbols in fig.6, also reflect the bimodal distribution of the massive podiform chromite. The massive chromite with the higher content of Cr_2O_3 is associated with olivine while that with the higher percentage of Al_2O_3 is associated with enstatite, clinopyroxene, and feldspar. The high-chromium chromite never occurs with enstatite or feldspar and only with minor, interstitial diopside.

Olivine compositions--The olivine analyzed in this study is typically high in forsterite. The average values are near Fo92 for olivine associated with low chromium, high-aluminum chromite, enstatite, diopside, and feldspar and Fo94-95 for olivine associated with high-chromium chromite and minor diopside (Bird, 1977).

The range of the forsterite molecule in olivine associated with the high-chromium chromite in the massive layers of the Red Mountain complex, however, is about Fo92-Fo97. The accessory and other high-aluminum chromite at Red Mountain is associated with olivine having a forsterite content of Fo85-Fo92.

Pyroxene compositions--The pyroxenes from the alpine chromitites in this study are largely diopsides with some enstatite or bronzite. The diopsides generally contain 1-4% FeO (total Fe oxide), 0-.5% Na2O, 0.3-4% Al2O3, 0-1% TiO2, and 0-2% Cr2O3.

The Al2O3 content varies reciprocally with SiO2 indicating substitution of Al3+ in the Si tetrahedron. Where Al is abundant it also is the dominant ion substituting in the octahedral sites for charge balance. This is especially true where the diopside is associated with high alumina chromite. Diopside associated with high-chromium chromite generally does not contain sufficient Al to fill tetrahedral sites not occupied by Si and the ions Fe3+, Ti4+, and possibly Cr3+ are assumed to fill the remaining sites.

There is positive correlation between the Cr/Al ratio in pyroxenes and associated chromite. The plot of (Cr/Al)di vs (Cr/Al)ch shows a break between high-Al and high-Cr chromites at (Cr/Al)ch = 2.2 to 2.3 (molar ratio) corresponding to a Cr content in the high-Cr chromite in excess of 1.3-1.4 moles (fig.10).

The pyroxene enstatite associated with diopside and high alumina chromite contains 2 to 3 times as much FeO as does the diopside while its content of Al2O3 is equal to or about one-half that of diopside. The Al2O3 content

of the enstatite ranges from 0.6 to 2.3 weight per cent. Both enstatites and diopsides associated with feldspars, e.g. Cuban chromitites, are higher in Al_2O_3 and Na_2O.

Iron-Magnesium distribution coefficient, Kd, between olivine and chromite in alpine complexes--It has been shown by various authors that olivine (Sahama and Torgeson, 1949; Schwerdfeger and Muan, 1966; Nafziger and Muan, 1967; and Williams, 1972) and chromite (Irvine, 1965) can be treated as approximately ideal solid solutions; that is, the activity coefficients for iron and magnesium are approximately unity. The iron-magnesium distribution coefficient, Kd, therefore approximates the equilibrium constant for the exchange reaction of Fe and Mg between chromite and olivine and can be written as

Kd =

where is the activity coefficient of Fe in olivine, X is the mole fraction of Fe in olivine, (Fe/Mg)ol is the mole ratio of iron and magnesium in olivine, etc. (Jackson, 1969). The values m and b are the slope and ordinate intercept, respectively, on the plot of (Fe/Mg)ol vs (Fe/Mg)ch.

Treating olivine and chromite as ideal solid solutions at constant temperature and pressure, the graph of (Fe/Mg)ol plotted against (Fe/Mg)ch is found to be linear and have a zero intercept. The slope of the line, therefore, gives the value of the distribution coefficient, Kd.

The partial pressure of oxygen during the crystallization of alpine-type ultramafic rocks was very low and essentially constant (Irvine, 1967). Similarly, the pressure can be treated as constant since the entire range of composition occurs in only a few feet of stratigraphic section and the volume change involved in the reaction is small (Irvine, 1965). It can be assumed, therefore, that the constant value of Kd determined for high-chromium alpine-type chromite-olivine associations around the world reflects uniformity in the temperature of crystallization (or recrystallization) for these rocks.

Sinton (1976) has suggested that a constant distribution coefficient of elements between two phases indicates a constant temperature of equilibration (probably metamorphic) and the variation in composition of the phases reflects variation in composition between layers.

Figure 11 is a graph of the Fe2+/Mg ratios for all olivine-chromite pairs analyzed in this study with the exclusion of the Red Mountain, Alaska complex. The solid circles (dots) represent all of the high-chromium chromitites and the open circles represent the high-alumina chromites. The outstanding feature of the graph is the linear relationship shown by the high-chromium chromite-olivine pairs (solid circles). The average chromic oxide value of the chromite along this line is 54 per cent. This is the same average obtained for the high-chromium chromite in the histogram of fig.9a. The chromite with an Fe2+/Mg ratio which varies linearly with that of olivine and that in the high-chromium mode of the histograms represent the same population. The graph of fig.11 has a slope of approximately .05 and an intercept near zero. Therefore, the value of Kd is approximately .05.

The constant value of Kd suggests that all of the high-chromium chromite and associated olivine crystallized or equilibrated at about the same temperature.

It is significant that the data along the line for which Kd = .05 comes from widely separated alpine complexes scattered from around the world.

Figure 12 shows the graph of (Fe/Mg)ol plotted against (Fe/Mg)ch for the chromitites of the Red Mountain complex, Seldovia, Alaska. The Fe/Mg ratios vary from 0.45 to 2.30 for chromite and from 0.02 to 0.12 for olivine. Similar to the graph of the other alpine complexes (fig.11) the data for the high-chromium chromite and associated olivine describe a linear relationship between points A and B and have an intercept near the origin. The nearly constant value of Kd determined from the slope of the graph is 0.046 closely corresponding to the value of .05 determined from the data for other olivine chromitites.

The graphed data between points B and C of fig.12 correspond to accessory chromite and high-alumina chromite associated with anorthitic dikelets (circled points). This section of the graph shows a variation of the distribution coefficient, Kd, with composition of the chromite. The variation of the data along the line (Fe/Mg)ol = -.0036(Fe/Mg)ch + .105 between the ordinate and the intersection with the line for which Kd is .046 suggests a general locus of points for all high-alumina chromite. Data for massive high-alumina chromite deposits also lie near this line but are too few to define a trend.

Comparison of alpine-type chromitite with stratiform chromitite and chromite from recent lavas-- Studies of the stratiform ultramafic complexes convincingly demonstrate tnat magmatic differentiation has occured in them. Jackson (1969, 1970) and Irvine (1970) have shown that in the crystallization of a magma from which a stratiform-type chromite deposit is derived, magnesian olivine crystallizes and accumulates together with high-chromium, high-magnesium chromite. The differentiation trend, as determined from the changes in chromite composition, is from high-chromium, low-iron to low-chromium, high-iron chromite. As the iron increases in the chromite the iron content of the olivine also increases with continuing differentiation. In general, the aluminum content of the chromite also increases as the chromium decreases. Figure 13 shows the graph of Cr/(Cr+Al+Fe3+) plotted against Mg/(Mg+Fe2+) for the chromite from the G and H chromitite zones of the Stillwater stratiform complex, Montana. The chromite of both zones decreases in chromium and increases in iron from bottom to top. Similar graphs have been made in other studies of stratiform chromite (Thayer, 1970). All show the same trend as does fig.13 with chromic oxide and magnesium oxide decreasing as ferrous oxide increases. This trend is identical with that illustrated

for massive high-chromium chromite of Red Mountain, Alaska shown in fig.7. No trend in chromite composition comparable to the alpine trend, however, is observed for the stratiform chromite nor for tne chromite in the Hawaiian lavas (Evans et al, 1972).

Variations in the chromite compositions from the H chromitite zone of tne the Stillwater complex are illustrated by fig.13 to snow the increase in magnesia and decrease in alumina as chromium increases. The variations are monotonic and are comparable to those of the high-chromium alpine chromite but change at a different rate. Similar variations of iron and magnesium are shown in fig.14 for the Hawaiian chromite.

Recent microprobe studies of lavas and peridotite samples from the mid-Atlantic ridge by the author (unpublished data) have demonstrated that the alpine trend, as defined by the graph of Cr/(Cr+Al+Fe3+) plotted against Mg/(Mg+Fe2+), is characteristic of those rocks also. The work of Sigardson and Schilling (1976) has also shown the same alpine variation to exist in ultramafic rocks from the mid-Atlantic ridge.

Comparison of the iron-magnesium distribution coefficient between cnromite from stratiform complexes (and Hawaiian lavas) and alpine chromitites also shows differences between the two types. Figure 15 shows the graph of (Fe/Mg)ol plotted against (Fe/Mg)ch for the G and H chromitite zones of the Stillwater complex and the Hawaiian lavas. The trend of the alpine high-chromium chromite data is shown for comparison.

Similarity between the Stillwater G and H zones data and the Hawaiian lava data are shown by the slopes of the graph. The slopes of the three lines are approximately 0.135 compared to values near .05 for alpine chromitites.

For the alpine and the H zone chromitites the value of the intercept b, is approximately zero and Kd is .05 and .135 respectively. For the two remaining graphs the intercept does not equal zero and Kd varies with the composition of the chromite. The similarities between chromite from the G and H zones and the Hawaiian lava chromite and the differences of the alpine chromite are apparent.

The iron-magnesium distribution coefficient data from the mid-Atlantic ridge (Sigardson and Schilling, 1976), however, show similarities to the stratiform and Hawaiian chromite instead of to the alpine chromitites.

The occurrence of chromite, in lavas of the mid-Atlantic ridge, having a range in chromite composition which defines the alpine trend but having an Fe-Mg distribution coefficient between it (chromite) and olivine which is similar to the distribution coefficient of stratiform chromitites suggest that composition of the magma determines the alpine trend and that pressure is a major factor in determining the distribution coefficient.

Summary and conclusions

The massive chromite deposits which are present in alpine-type ultramafic complexes are bimodal with respect to their chromic oxide content. The two modes are at 37 $\pm$ 3 per cent and 54 $\pm$ 4 per cent chromic oxide corresponding to refractory grade and metallurgical grade chromite respectively. Alpine chromites, therefore, have a natural break in chromic oxide content between these two grades.

The high-chromium, low-magnesium to low-magnesium to low-chromium, high-magnesium trend shown by the graph of Cr/(Cr+Al+Fe3+) plotted against Mg/(Mg+Fe2+) for the alpine chromite is termed the alpine trend. It is a distinguishing feature which differentiates between alpine and stratiform type chromitites.

The data from Red Mountain, Seldovia, Alaska illustrate that alpine chromite also has a high-chromium chromite trend which is comparable to that for stratiform chromite. In alpine chromitite, however, the Fe/Mg distribution coefficient between high-chromium chromite and the associated olivine has a distinctive value of approximately .05 compared to .135 for stratiform chromitites. An Fe/Mg distribution coefficient between high-chromium chromite and olivine of approximately .05 is, therefore, a second distinguishing feature of alpine chromitites.

Each of the two modes of chromite is associated with its characteristic suite of silicate minerals. The high-chromium chromite is associated with highly magnesian olivine and minor diopside. The high-aluminum chromite is associated with more ferrous olivine, enstatite, diopside, and feldspar and usually occurs at the top of the ultramafic section adjacent to gabbro.

The occurrence of two distinct types of chromite deposits in alpine ultramafic complexes, each with its characteristic range in composition, associated suite of silicate minerals, and distinctive iron-magnesium distribution coefficient between the chromite and olivine suggests two different populations of chromite with different modes of origin.

Continuous differentiation from the high-chromium to the high-aluminum chromite may also be postulated. Supporting this latter view is the fact that when gabbro immediately overlies the ultramafic section, chromite in the ultramafics adjacent to the gabbro is high in alumina and the high-chromium chromite occurs in the dunite further away from the gabbro. Interpreting the dunite-gabbro relationship as representing a stratigraphic succession with gabbro at the top, the decrease in chromium content of the chromite and increase in the iron of the olivine and pyroxene indicate a sequence of continuing differentiation. However, if differentiation is the controlling method by which the composition of the chromite is varied, one might expect to find a continuous range in chromite composition from the the high-chromium chromite in the dunite to the high-aluminum chromite adjacent to the gabbro. Instead, two populations of chromite are found.

Continuous variation does occur in the accessory chromite but not in the massive ore bodies. In general, the high-aluminum chromite grains occur only as accessories except in podiform deposits and other small concentrations adjacent to feldspathic intrusives.

In lieu of the hypothesis of continuous differentiation it is postulated that the massive deposits of the high-aluminum chromite result from metamorphic reaction and recrystallization of the uppermost part of the ultramafic section and its contained chromite with the overlying gabbro section serving as a source of aluminum. In support of this hypothesis, the high-aluminum chromite pods, which frequently contain a feldspathic gangue, occur within a sheath consisting of an inner zone of dunite and an outer zone of orthopyroxene deficient harzburgite adjacent to the gabbroic rocks. The zoning, which is usually present, suggests a reaction between the gabbro and ultramafic rocks.

The chromite and associated silicate minerals in the pods of high-alumina chromite almost always contain textural relationships such as armored relics of olivine encased by chromite and both ortho- and clinopyroxene which can be interpreted as having been formed by metamorphic reaction and recrystallization. The chromite and pyroxene generally lie between the olivine and enclosing feldspar. If this hypothesis is correct then some of the ore bodies of high-aluminum chromite should show internal variations from the high-chromium to the high-aluminum chromite. Reported chemical analyses from some of the deposits indicate that this variation does occur although no detailed work has been done on a single deposit. Similarly, many hand specimens containing composite grains in which euhedral crystals of chromite are enclosed by anhedral chromite of much lower chromium content have been observed in this investigation.

Comparison of the high-chromium alpine chromitite data with data from stratiform chromitites suggest that the two had similar origins by precipitation from a magmatic melt. Comparisons with analytical data from recent lavas suggest that some of the differences between the stratiform and alpine types are due to differences in compositions of the melts from which they were derived.

The presence of high-aluminum chromite bodies in the uppermost part of the ultramafic section and the high-chromium chromite bodies in the lower parts of the ultramafics suggest that areas which contain high-aluminum chromite such as the Camaguey chromite district, Cuba might contain metallurgical grade chromite more distant, either laterally or vertically, from the dunite-gabbro contact.

References cited

Bird, M.L., 1977, Electron microprobe analyses of chromite and associated silicate minerals from alpine ultramafic complexes: U.S. Geol. Survey open file rept. 77-236.

Coleman, R.G., 1971, Plate tectonic emplacement of upper mantle peridotites along continental edges: J.Geophys. Res., 76, 1212-1221.

Davies, H.L., 1971, Peridotite-gabbro-basalt complex in eastern Papua; an overthrust plate of oceanic mantle and crust: Australian Bur. Min. Res., Bull. 128, 48.

Dewey, J.F., and Bird, J.M., 1970, Mountain belts and the new global tectonics: J.Geophys. Res. 75, 2625-2648.

Evans, B.W., and Wright, T.L., 1972, Composition of liquidus chromite from the 1959 (Kilauea Iki) and 1965 (Makaopuki) eruptions of Kilauea volcano, Hawaii: Amer. Mineral.57, 217-230.

Flint, D.E., de Albear, J.F., and Guild, P.W., 1948, Geology of chromite deposits of the Camaguey district, Camaguey Province Cuba: U.S. Geol. Survey Bull. 954-B, 39-63.

Golding, H.G., and Bayliss, P., 1968, Altered chrome ores from the Coolac serpentine belt, New South Wales, Australia: Amer. Mineral. 53, 162-183.

Golding, H.G., and Johnson, K.R., 1971, Variation in the gross chemical composition and related physical properties of podiform chromite in the Coolac district, N.S.W., Australia: Econ. Geol. 66, 1017-1027.

Irvine, T.N., 1965, Chromian spinel as a petrogenetic indicator, pt. 1 Theory: Can. J. Earth Sci. 2, 648-672.

----------, 1967, Chromian spinel as a petrogenetic indicator, pt. 2, Petrologic applications: Can. J. Earth Sci. 4, 71-103.

----------, 1970, Crystallization sequences in the Muskox intrusion: Symposium on the Bushveld Igneous Complex and other layered intrusions: Geol. Soc. Africa, Spec. Pub. no.1, 441-476.

Irvine, T.N., and Findlay, T.C., 1971, Alpine-type peridotite with particular reference to the Bay of Islands igneous complex: Canadian Contribution No. 8 to the Geodynamics Project.

Jackson, E.D. , 1969, Chemical variation in coexisting chromite and olivine in chromite zones of the Stillwater Complex: Econ. Geol. Mon. 4., Magmatic Ore Deposits, (ed. H.D.B. Wilson), 41-71.

----------, 1970, The cyclic unit in layered intrusions - a comparison of repetitive stratigraphy in the ultramafic parts of the Stillwater, Muskox, Great Dyke, and Bushveld complexes: Symposium on the Bushveld Igneous complex and other layered intrusions: Geol. Soc. South Africa, Spec. Pub. no. 1, 1970, 425-440.

Jackson, E.D., Green, H.W., and Moores, E.M., 1974, The Vourinos Ophiolite, Greece; Cyclic units of lineated cumulates overlying harzburgite tectonite: Bull. Geol. Soc. Amer. 86, 390-398.

Lanphere, M.A., 1973, Strontium isotopic relations in the Canyon Mountain, Oregon and Red Mountain, California ophiolites: Abst. Amer. Geophys. Union Trans. 54, no. 11, 1220.

Loney, R.A., Himmelberg, G.R., and Coleman, R.G., 1971, Structure and petrology of the alpine-type peridotites at Burro Mountain California, U.S.A.: J. Petrol. 12, 245-309.

Malpas, J., and Strong, D.F., 1975, A comparison of chrome-spinels in ophiolites and mantle diapirs of Newfoundland: Geochem. Cosmochim Acta 39, 1045-1060.

MacGregor, I.D., and Smith, C.H., 1962, The use of chrome spinels in petrographic studies of ultramafic intrusions: Can. Contrib. to Internat. Upper Mantle Project No. 4.

Moores, E.M., 1969, Petrology and structure of the Vourinos complex of Northern Greece: Geol. Soc. Amer. Spec. Paper 118.

NMAB, 1970, Trends in usage of chromium: National Materials Advisory Board Rept. 256, National Research Council, Washington, D.C.

Rossman, D.L., Fernandez, N.S., Fontanas, C.A., and Zepeda, Z.C., Chromite deposits on insular chromite reservation number one, Zambales, Philippines: Bureau of Mines, Philippines Special Project Series, Pub. No.19-Chromite.

Rossman, D.L., 1970, Chromite deposits of the north-north-central Zambales Range, Luzon, Philippines, U.S. Geol. Survey open file rept. 1390, 1-65.

Sahama, Th. G., and Torgeson, D.R., 1949, Some examples of the application of thermochemistry: J. Geol. 57, 255-262.

Sampson, Edward, 1929, May chromite crystallize late: Econ.Geol.24, 632-649.

----------, 1931, Varieties of chromite deposits: Econ.Geol. 26, 833-839.

----------, 1932, Magmatic chromite deposits in southern Africa: Econ. Geol. 27, 113-144.

Schwerdfeger, K., and Muan, A., 1966, Activities in olivine and pyroxenoid solid solutions of the system Fe-Mg-Si02 at 1150 C: Trans. Metall. Soc. AIME. 236, 201-211.

Sigardson, H., and Schilling, J.G., 1976, Spinels in mid-Atlantic ridge basalts: Chemistry and occurrence. Earth Planet. Sci. Lett. 29, 7-20.

Sinton, John M.,1977, Equilibration History of the Basal Alpine-Type Peridotite, Red Mountain, New Zealand; J. Pet. 18, pt.2, 216,246.

Smitn, C.H., 1958, Bay of Island Complex, Western Newfoundland Geol. Survey of Can. Memoir 290, 1-131.

Stoll, W.C., 1958, Geology and Petrology of the Masinloc Masinloc chromite deposit, Zambales, Luzon, Philippine Islands, Bull. Geol. Soc. Amer. 69, 419-448.

Sweatman, T.R., and Long J.V.P., 1969, Quantitative electron-probe microanalysis of rock-forming minerals: J.Pet. 10, 332-379.

Thayer, T.P., 1942, Chrome resources of Cuba: U.S.Geol. Survey Bull. 935-A, 1-74.

----------, 1949, Preliminary chemical correlation of chromite with the containing rocks: Econ. Geol. 61, 202-217.

----------, 1956, Preliminary geologic map of the John Day quad., Oregon: U.S. Geol. Survey Min. Map No. 51.

----------, 1963, Geologic features of podiform chromite deposits; Methods of Prospecting for chromite seminar: Athens, 135-148.

----------, 1969, Gravity differentiation and magmatic re-emplacement of podiform chromite deposits. In Wilson, H.B.D., ed., Symposium on magmatic ore deposts. Econ. Geol. Monograph 4, 132-146.

----------, 1970, Chromite segregations as petrogenetic indicators: Geol. Soc. South Africa, Spec. Pub.1, Symposium on the Bushveld Igneous complex and other layered intrusions.

Williams, R.J., 1972, Activity-composition relations in the Fayalite-Forsterite solid solution between 900 and 1300 at low pressures: Earth Planet. Sci. Lett. 15, 256-300.

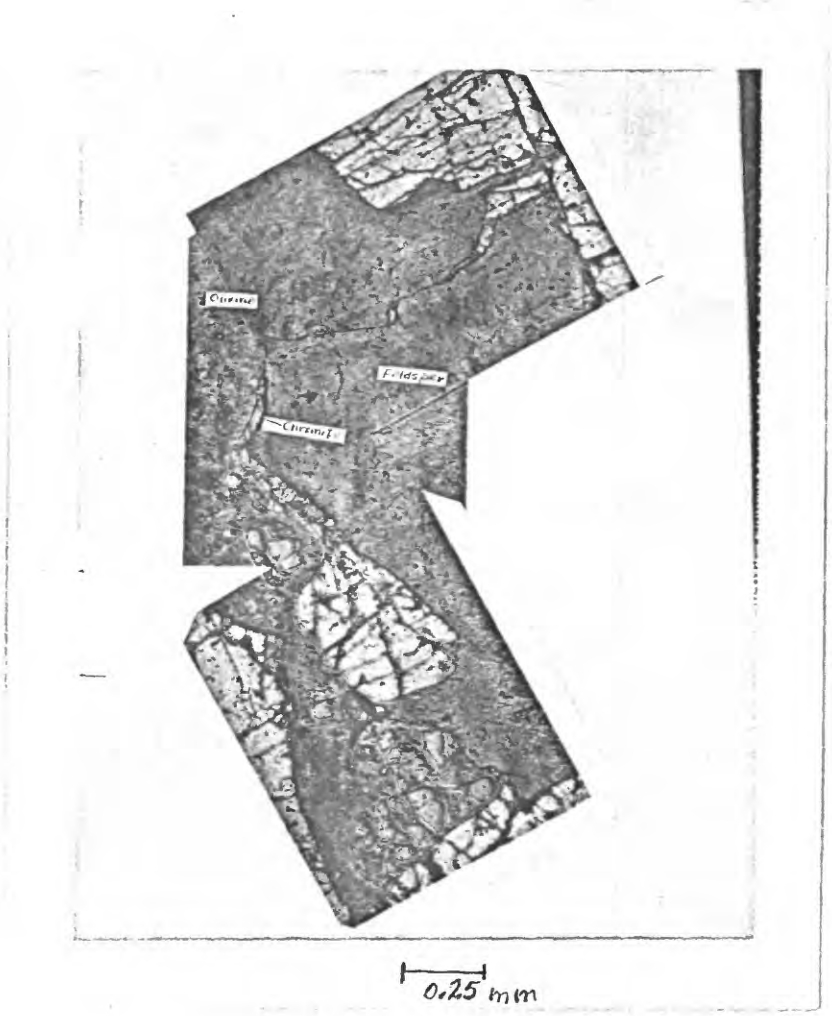

Fig. 1. Microphotograph of chromite hooks and stringers developed along olivine-feldspar interface. Note that pre-existing chromite appears to serve as a nucleating point for the stringers. Sample 42T50 from Camaguey, Cuba.

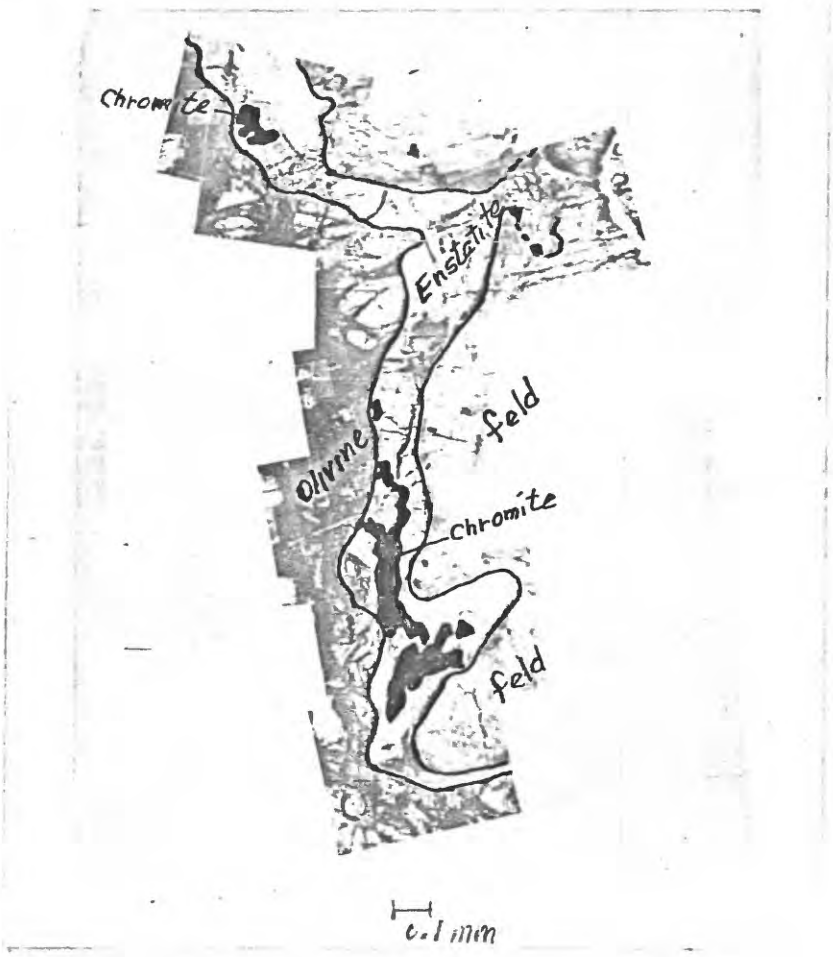

Fig. 2. Microphotograph of enstatite, diopside (not shown), and chromite in a reaction zone between olivine and pyroxene. Sample 42T49 from Camaguey, Cuba.

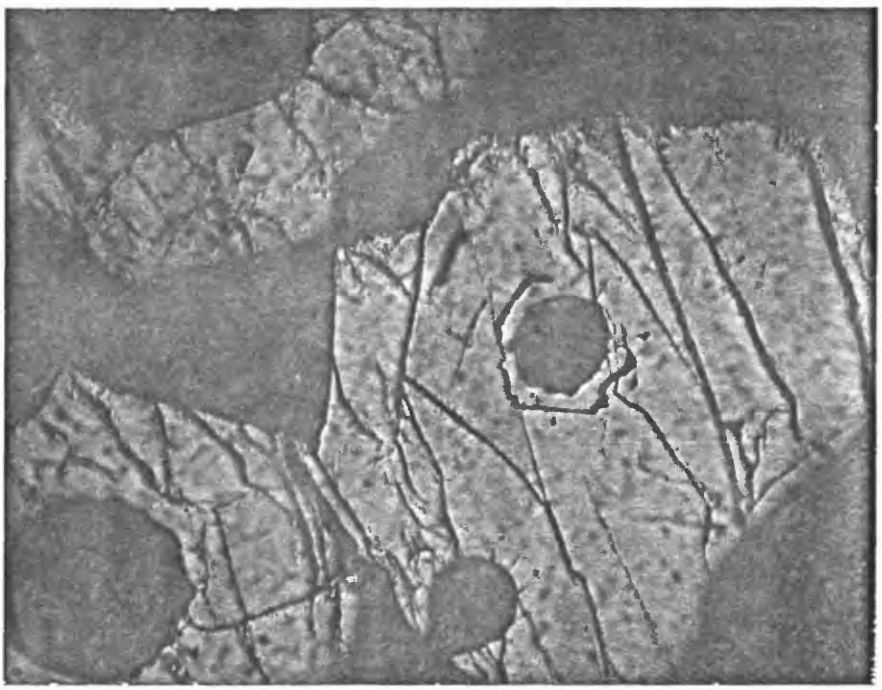

Fig. 3. Microphotograph of anhedral high alumina chromite (37% Cr2O) showing molding around olivine (serpentinized) and euhedral crystals (with serpentinized olivine centers) of higher chromium (44%) chromite serving as nuclei around which the chromite precipitated. Sample 59-P4 from the Coto mine, Philippine Islands.

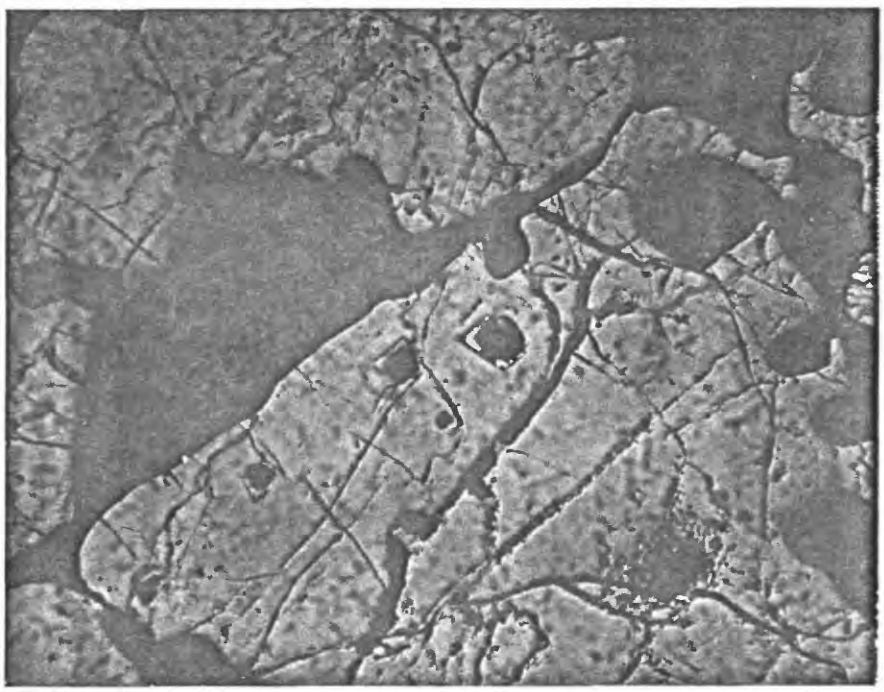

Fig.4. Microphotograph of anhedral high alumina chromite (36% Cr203) molded around olivine (serp.) and a higher chromium chromite (45% Cr203 crystal with olivine center. Sample 42T55 from Camaguey, Cuba.

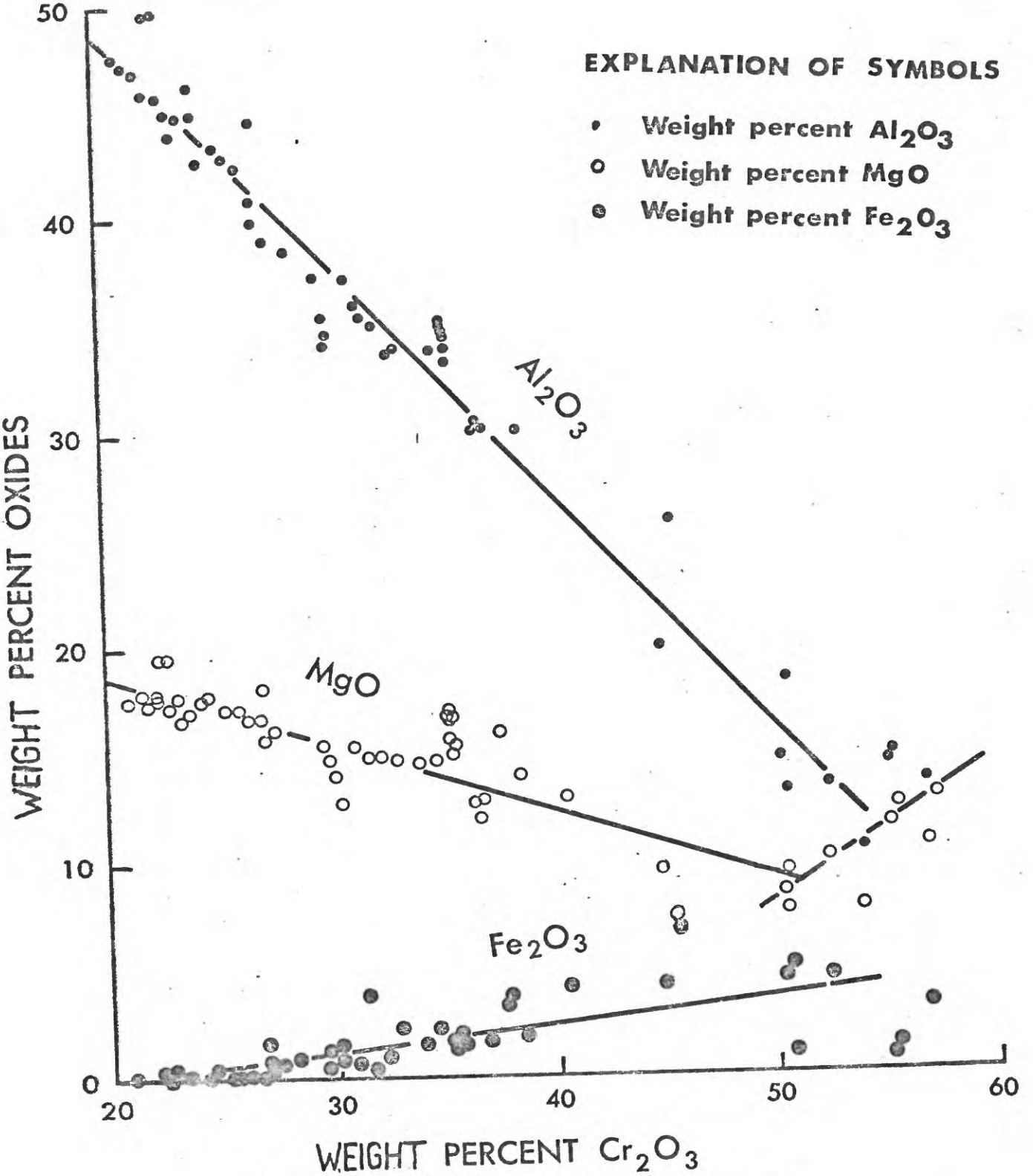

Fig.5. Variations in weight percent of Al203, MgO, and Fe203 in the alpine chromite at Red Mountain, Seldovia, Alaska as a function of Cr203 content. Magnesium oxide and ferrous oxide (not shown) sum to approximately 30 percent and vary reciprocally. Ferric and ferrous iron are calculated from total iron.

Fig.6. Graph of Cr/(Cr+Al+Fe3+) versus Mg/(Mg+Fe2+) for all high grade (massive) alpine chromite analyzed in this study. The graph illustrates the high-chromium to high-magnesium trend characteristic of alpine chromite and shows the bimodal distribution of the alpine chromite analyzed in this study. The silicate minerals associated with the analyzed chromite are indicated by symbols. Where only associated with serpentine the chromite composition is indicated by a dot. Multiple symbols indicate the presence of several silicate minerals.

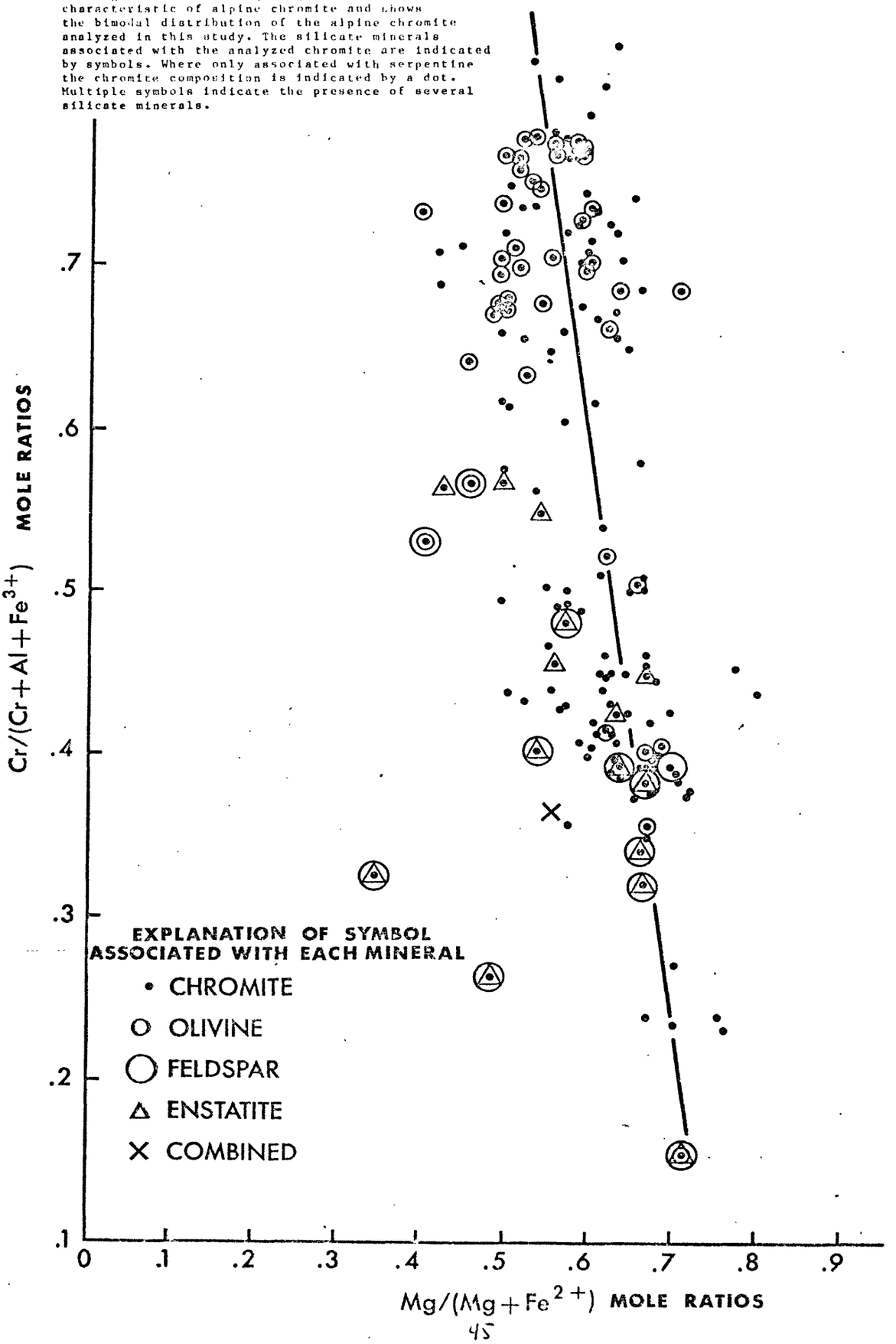

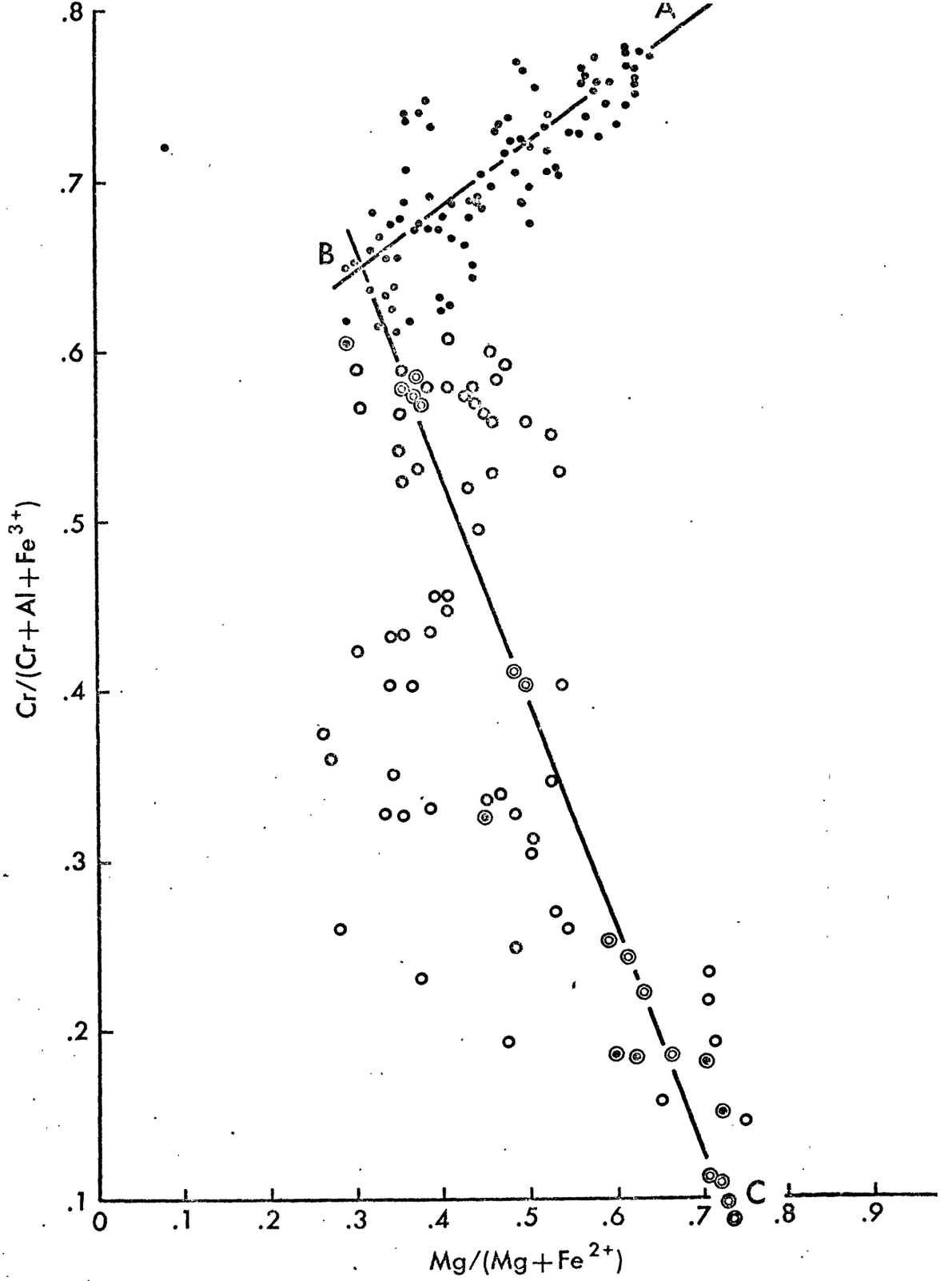

Fig.7. Graph of Cr/(Cr+Al+Fe7+) vs Mg/(Mg+Fe2+) for chromite of the Red Mountain alpine ultramafic complex at Seldovia, Alaska. The solid dots represent massive chromite, open circles show accessory chromite, double circles refer to accessory chromite in a continuous stratigraphic section, and circled dots represent apparently recrystallized chromite associated with anorthitic dikes.

The bimodality concept is not affected by the data on this graph since accessory chromite is included and bimodality refers only to massive deposits.

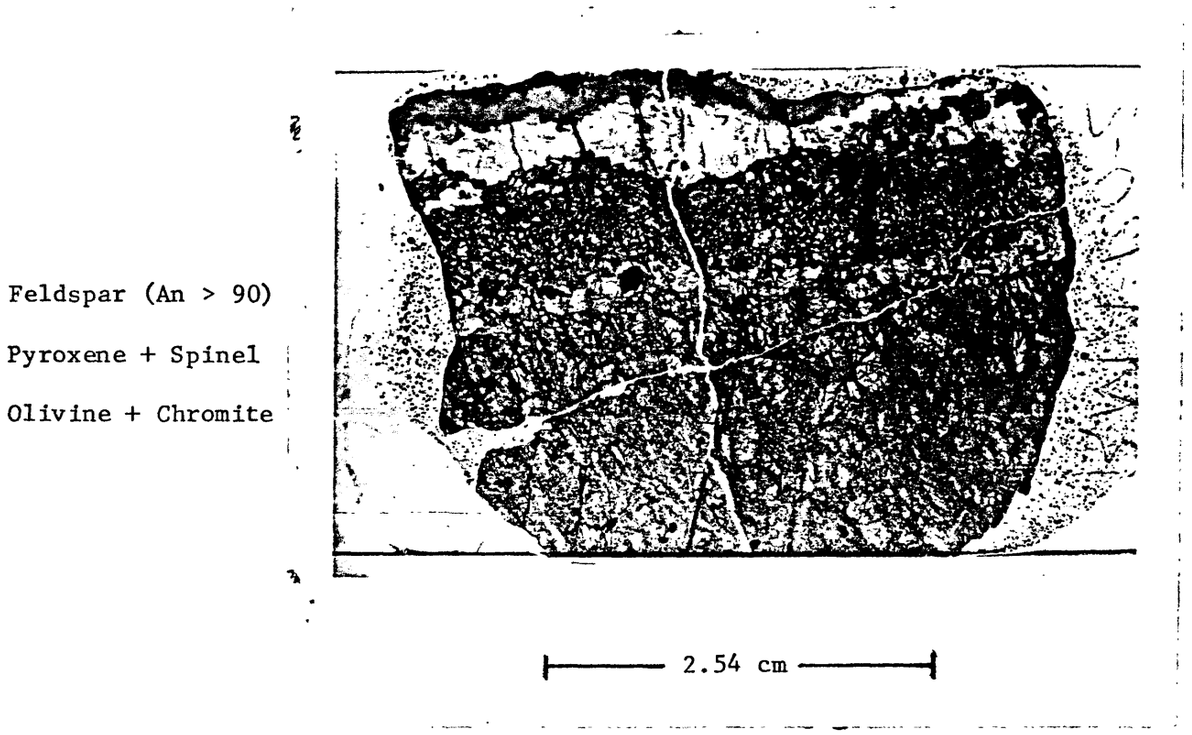

Fig.8. Photograph of specimen of olivine chromitite which has a reaction zone of pyroxene and spinel adjacent to an intrusive feldspar dikelet (white). The chromite grains (black) near the bottom of the section contain approximately 40% Cr_2O_3 while the large chromite grain (left center) near the reaction zone has less than 20% Cr_2O_3.

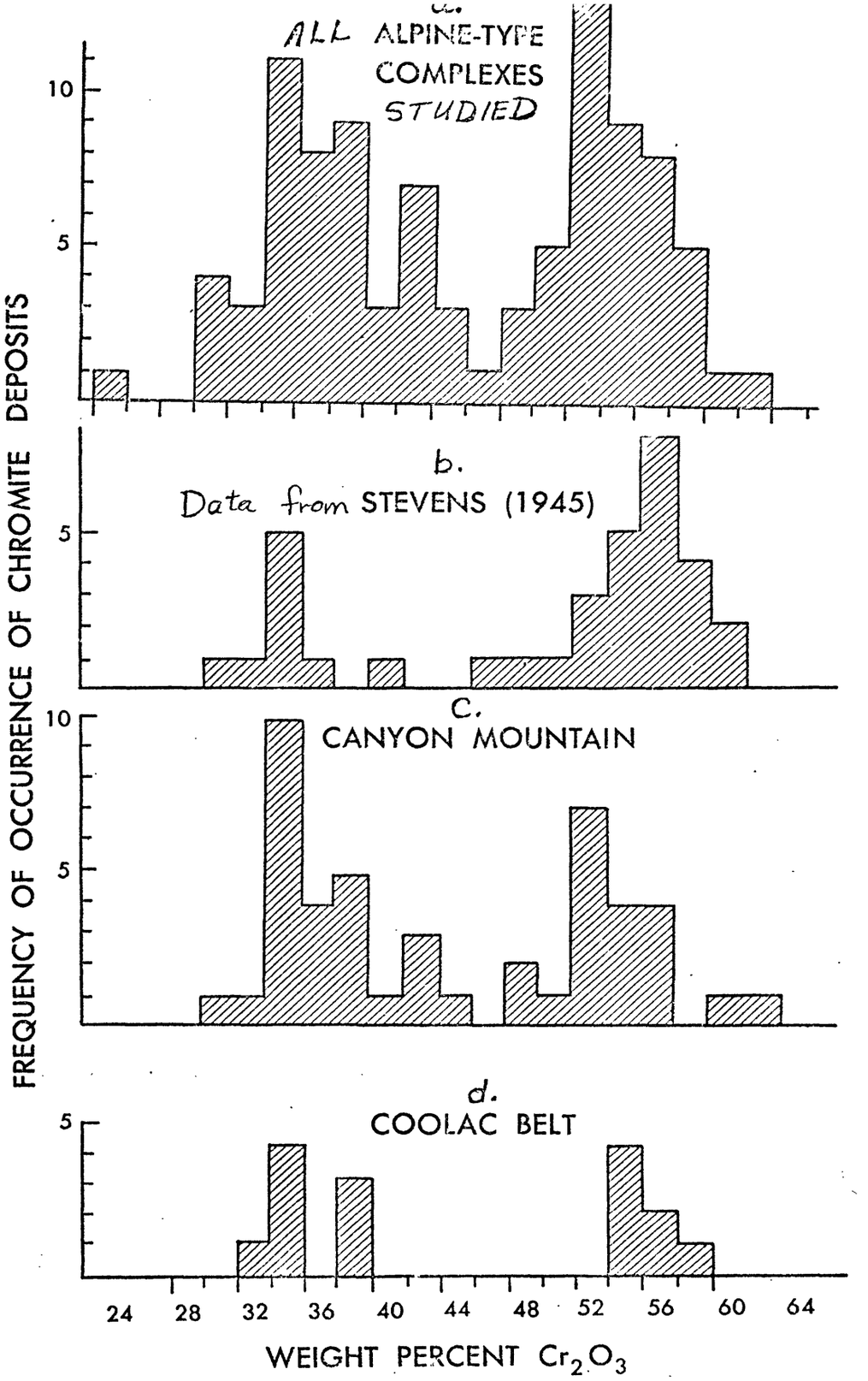

Fig.9. Histograms of the frequency of occurrence of alpine chromite deposits which contain chromite with different percentages of Cr203. The data for all alpine chromite deposits analyzed in this study are shown by 5a; data from Stevens (1945) are illustrated by 5b; data from the Canyon Mountain complex are shown in 5c; and the data for the Coolac Belt chromite analyzed in this study are shown in 5d. Each point plotted in the figure represents a chromite deposit or concentration. Alpine chromite deposits, including those from individual complexes, have two modes near 38 weight per cent and 54 weight per cent.

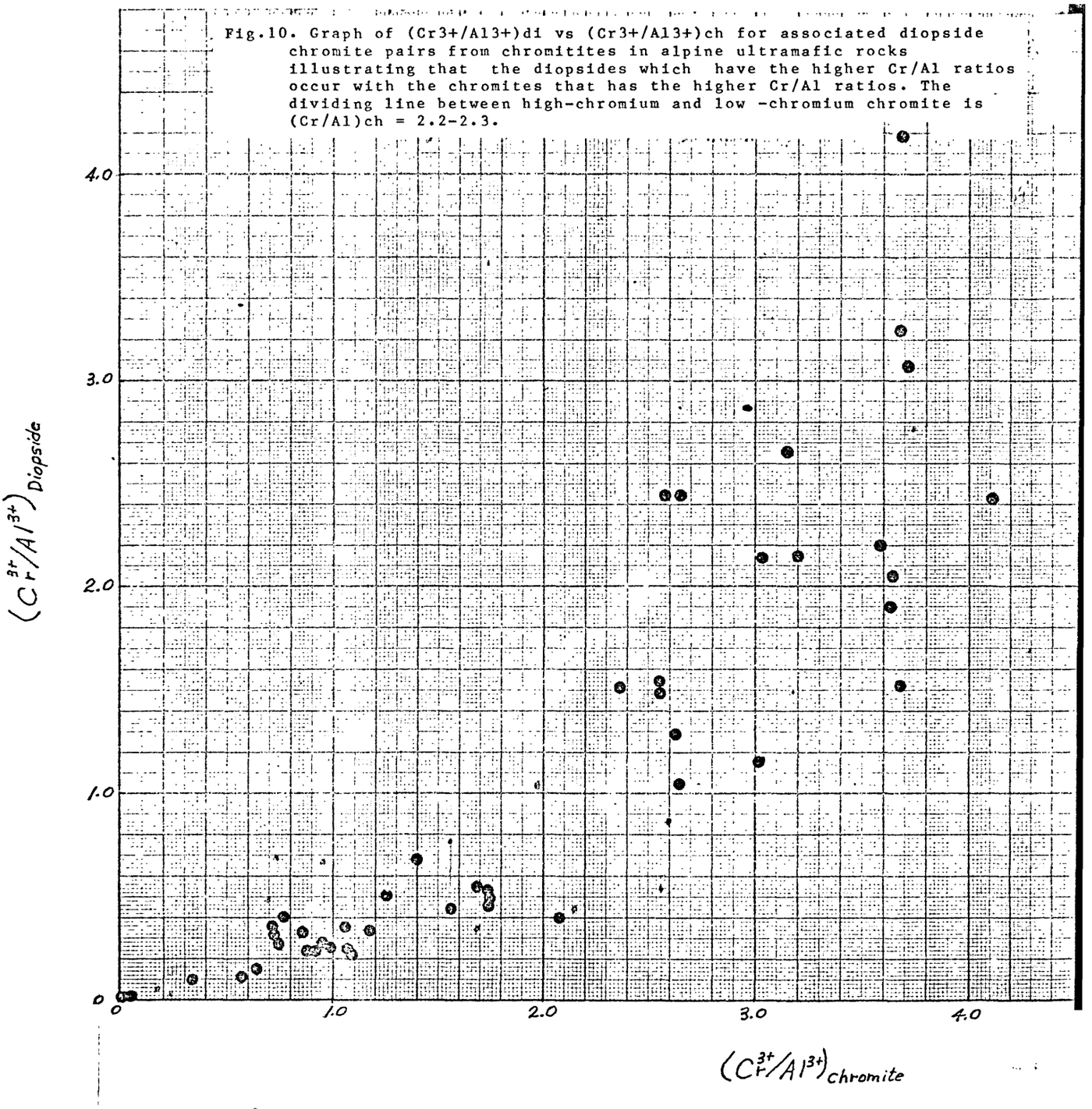

Fig.10. Graph of (Cr3+/Al3+)di vs (Cr3+/Al3+)ch for associated diopside chromite pairs from chromitites in alpine ultramafic rocks illustrating that the diopsides which have the higher Cr/Al ratios occur with the chromites that has the higher Cr/Al ratios. The dividing line between high-chromium and low -chromium chromite is (Cr/Al)ch = 2.2-2.3.

Fig.11. Graph of (Fe/Mg)ol versus (Fe/Mg)ch for all olivine-chromite pairs analyzed in this study with the exception of Red Mountain, Alaska. The solid dots represent high-chromium chromite-olivine pairs and the circled dots represent high-aluminum chromite-olivine pairs. The slope of the line drawn through the dots gives the value of Kd for the high-chromium-olivine pairs. The intercept value is approximately zero.

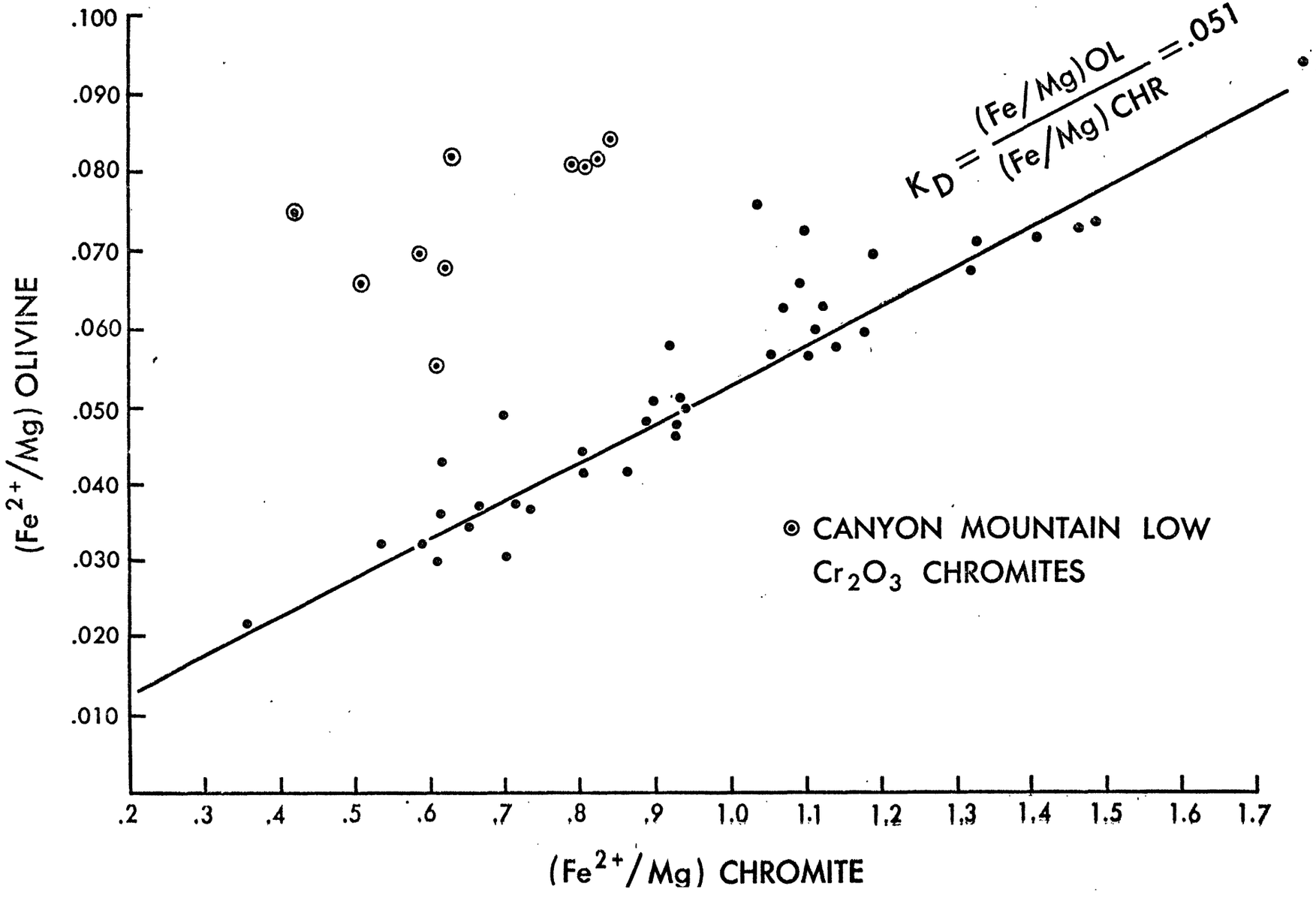

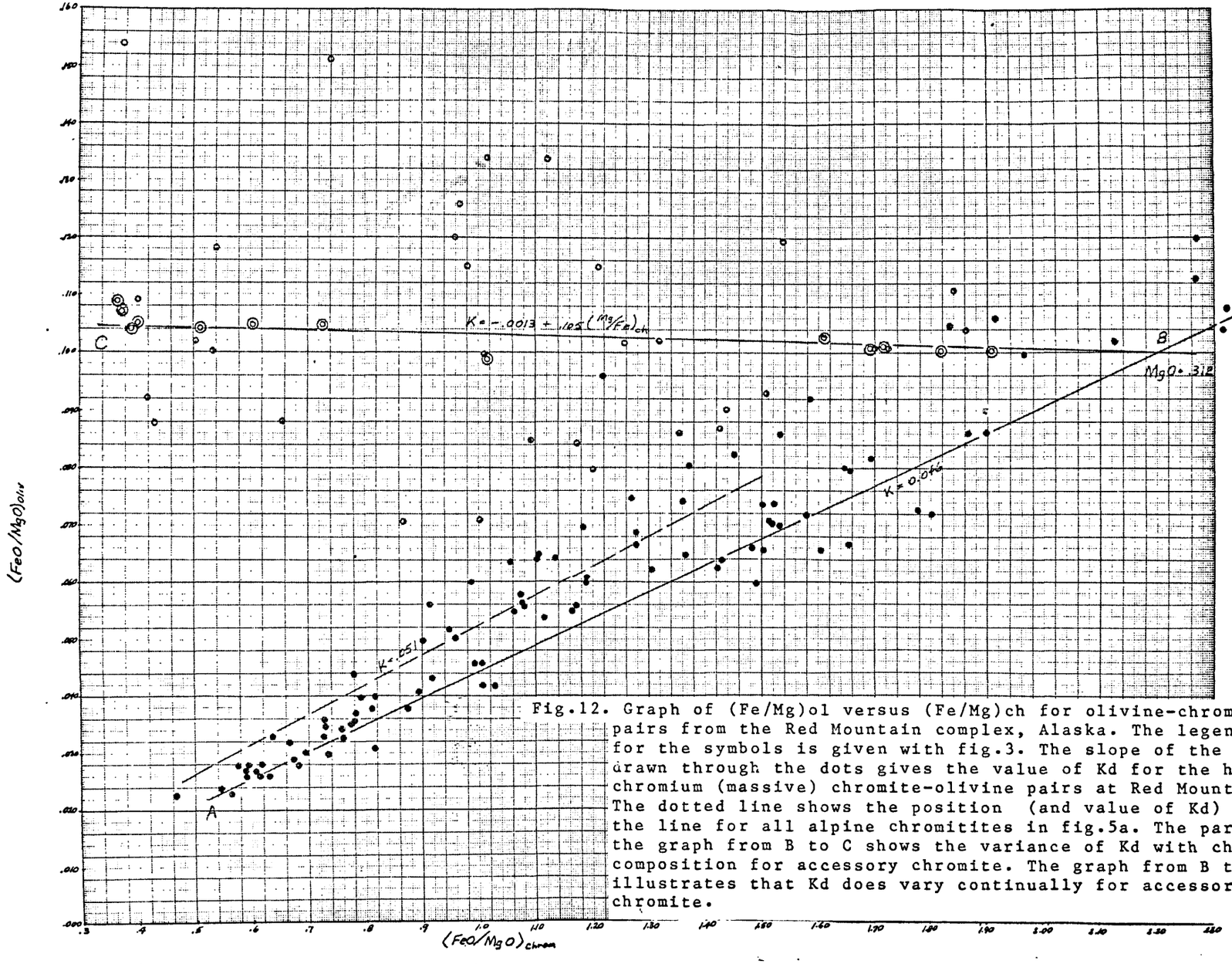

Fig.12. Graph of (Fe/Mg)ol versus (Fe/Mg)ch for olivine-chromite pairs from the Red Mountain complex, Alaska. The legend for the symbols is given with fig.3. The slope of the line drawn through the dots gives the value of Kd for the high-chromium (massive) chromite-olivine pairs at Red Mountain. The dotted line shows the position (and value of Kd) of the line for all alpine chromitites in fig.5a. The part of the graph from B to C shows the variance of Kd with chromite composition for accessory chromite. The graph from B to C illustrates that Kd does vary continually for accessory chromite.

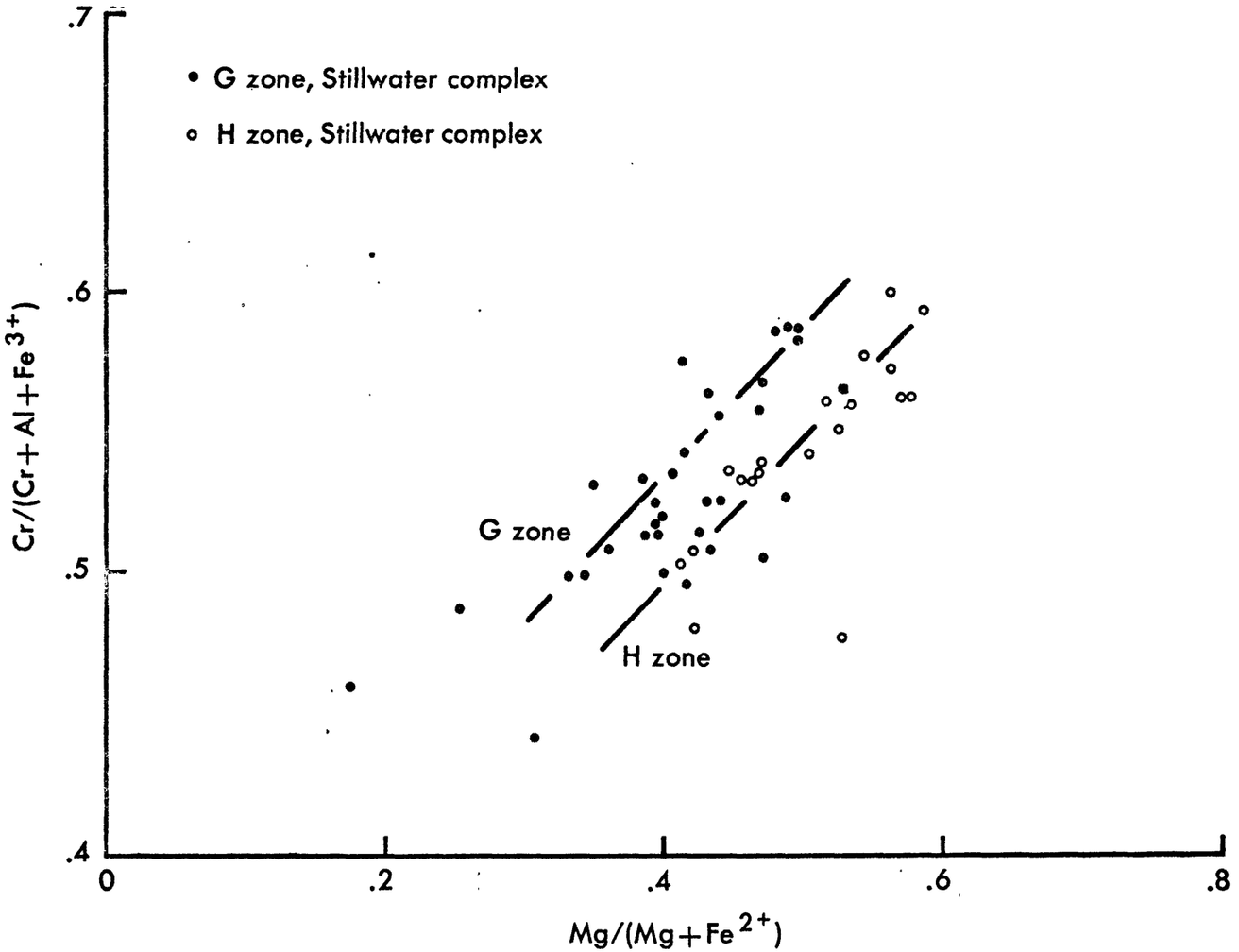

Fig.13. Graph of Cr/(Cr+Al+Fe3+) versus Mg/(Mg+Fe) for the stratiform chromite of the G and H chromitite zones of the Stillwater complex, Montana. The solid dots represent chromite in the G zone and circles chromite in the H zone. The trend from high-chromium, high-magnesium (top) to low-chromium, high-iron (bottom) is indicative of crystallization from a magmatic melt (Jackson, 1969). The graph illustrates the similarity of the stratiform trend to the high chromium-chromite trend of Red Mountain Alaska shown by the graph (A-B) in fig.3.

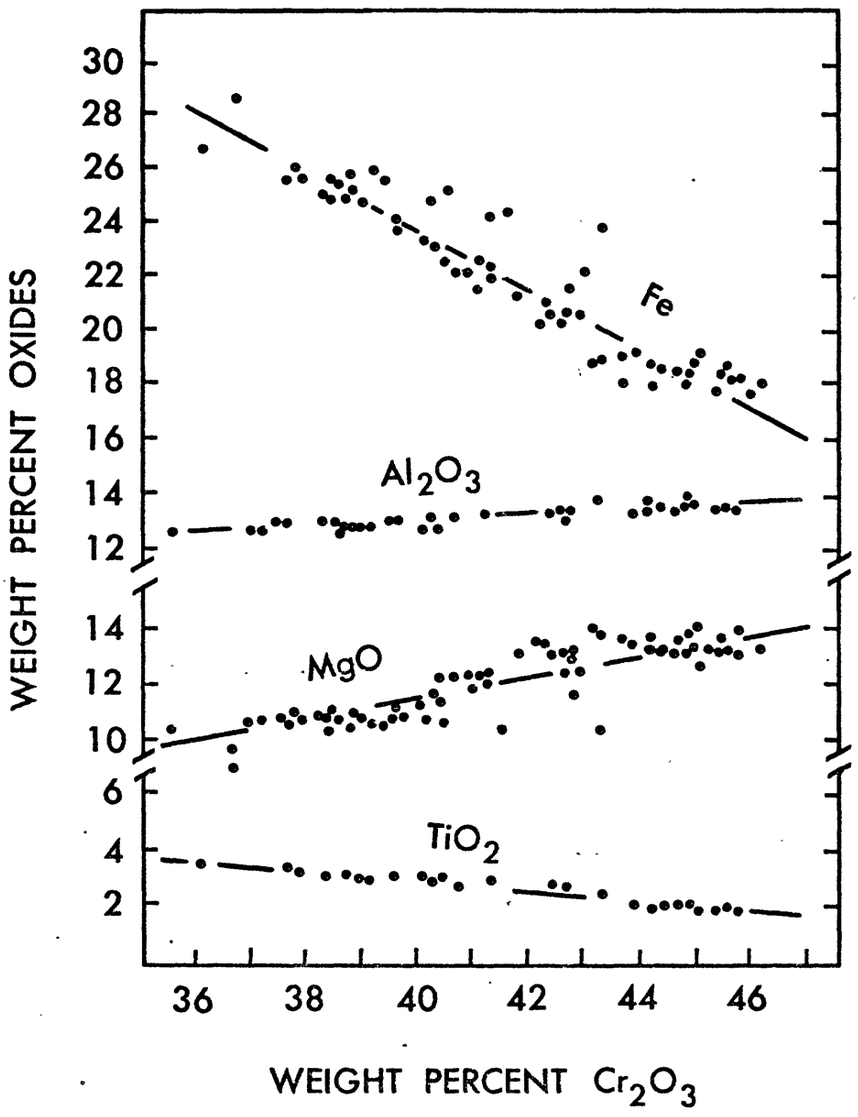

Fig.14. Compositional trends of individual chromite grains in the Hawaiian lavas.The increase in magnesium oxide as chromium oxide increases is similar to the trend in the Stillwater chromite but the increase in aluminum is anomalous. Data from Evans and Wright, 1972.

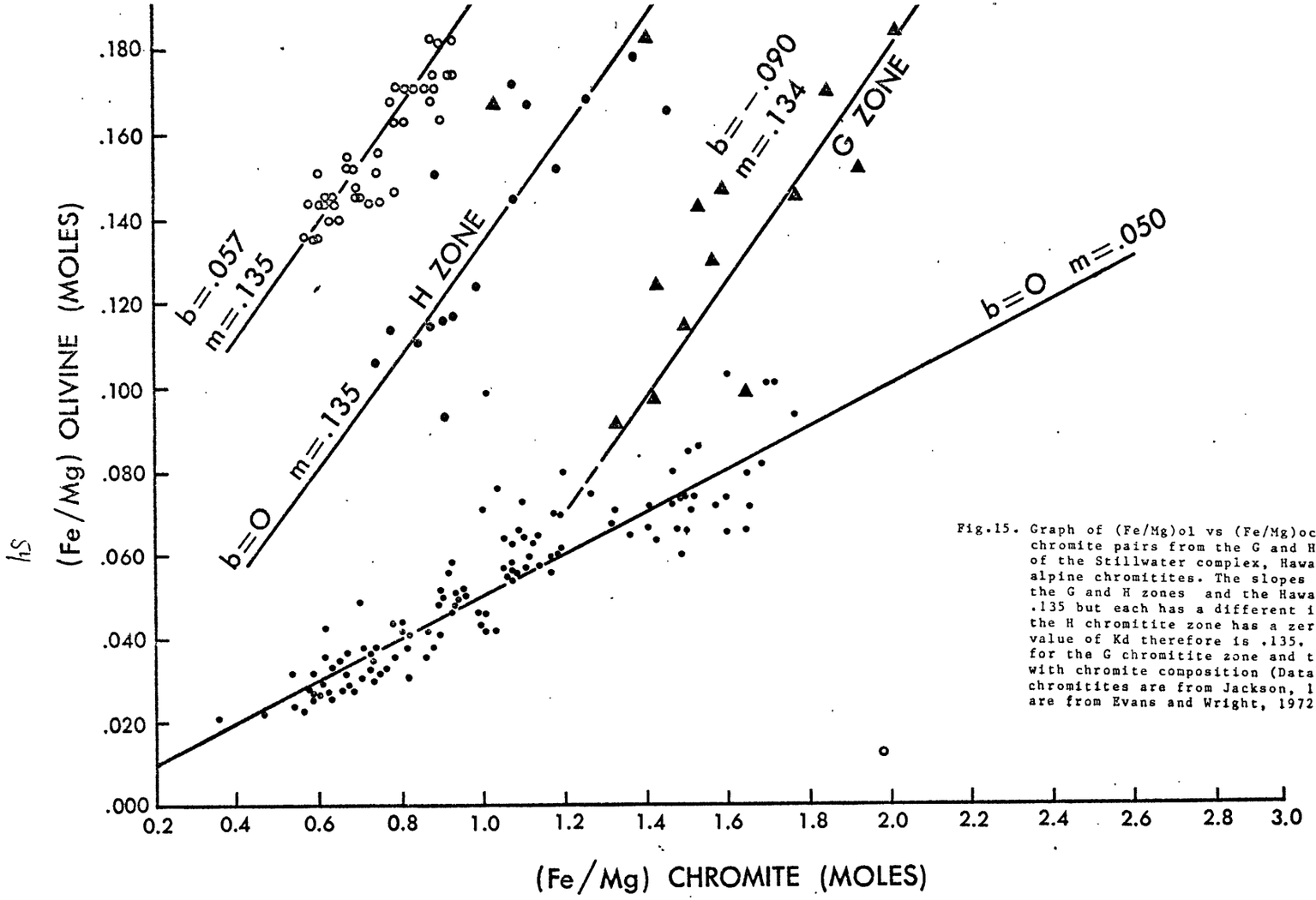

Fig.15. Graph of (Fe/Mg)ol vs (Fe/Mg)och for olivine-chromite pairs from the G and H chromitite zones of the Stillwater complex, Hawaiian lavas, and alpine chromitites. The slopes of the graphs for the G and H zones and the Hawaiian lavas is near .135 but each has a different intercept. The graph of the H chromitite zone has a zero intercept and its value of Kd therefore is .135. The values of Kd for the G chromitite zone and the Hawaiian lavas vary with chromite composition (Data for the Stillwater chromitites are from Jackson, 1969; data for Hawaiian are from Evans and Wright, 1972).